JOURNAL OF ENZYME INHIBITION AND MEDICINAL CHEMISTRY
2022, VOL. 37, NO. 1, 202–210
https://doi.org/10.1080/14756366.2021.1998024

Taylor & Francis
Taylor & Francis Group

RESEARCH PAPER

A polypeptide inhibitor of calcineurin blocks the calcineurin-NFAT signalling pathway *in vivo* and *in vitro*

Ping Wang[a*†], Wenying Li[a*], Yumeng Yang[a], Na Cheng[a], Yuchen Zhang[a], Nan Zhang[a], Yanxia Yin[a], Li Tong[a], Zhimei Li[b] and Jing Luo[a]

[a]Department of Biochemistry and Molecular Biology, Gene Engineering and Biotechnology of Beijing Key Laboratory, College of Life Sciences, Beijing Normal University, Beijing, China; [b]Department of Neurology, Beijing Tiantan Hospital, Capital Medical University, China National Clinical Research Center for Neurological Diseases, Beijing, China

ABSTRACT

Calcineurin (CN) controls the immune response by regulating nuclear factor of activated T cells (NFAT). Inhibition of CN function is an effective treatment for immune diseases. The PVIVIT peptide is an artificial peptide based on the NFAT-PxIxIT motif, which exhibits stronger binding to CN. A bioactive peptide (named pep4) that inhibits the CN/NFAT interaction was designed. Pep4 contains a segment of A238L as the linker and the LxVP motif and PVIVIT motif as CN binding sites. Pep4 has strong binding capacity to CN and inhibits CN activity competitively. 11-arginine-modified pep4 (11 R-pep4) inhibits the nuclear translocation of NFAT and reduces the expression of IL-2. 11 R-pep4 improves the pathological characteristics of asthmatic mice to a certain extent. The above results indicated that pep4 is a high-affinity CN inhibitor. These findings will contribute to the discovery of new CN inhibitors and promising immunosuppressive drugs.

ARTICLE HISTORY
Received 25 August 2021
Revised 12 October 2021
Accepted 17 October 2021

KEYWORDS
Calcineurin; NFAT; enzyme inhibitor; polypeptide

Introduction

Calcineurin (CN) is a serine/threonine protein phosphatase. It is widely distributed in various tissues, especially in nerve tissues and lymphocytes[1,2]. CN is a heterodimer composed of the catalytic subunit CNA and the regulatory subunit CNB. Its activity is regulated by Ca^{2+} and calmodulin (CaM). CN has a variety of substrates and plays an important role in various processes, including the immune response, autophagy and other biological systems[3]. T cell activating transcription factor (NFAT) is one of the substrates of CN. NFAT plays an important role in the development, activation and function of the immune system. In addition to T cells, NFAT is also expressed in a variety of other immune cells, regulating the expression of a variety of cytokines, such as IL-2, IL-3 and TNF α[4].

In the resting cytoplasm, NFAT is highly phosphorylated. When cells are activated, the intracellular calcium concentration increases, and Ca^{2+} binds to specific sites of CNB. CaM is also activated upon binding to calcium. Activated CNB and CaM change the conformation of CNA to expose active sites[3,5,6]. Activated CN dephosphorylates NFAT, and the nuclear localisation signal (NLS) of NFAT is exposed. Thus, NFAT is transported into the nucleus to regulate the expression of target genes. Given this important cascade event, the interaction between CN and NFAT is considered a T cell activation switch. Because of the important role of the CN/NFAT complex in regulating the immune response, it can be used as an important therapeutic target for immunosuppression[7–10]. Cyclosporin A (CsA) and tacrolimus (FK506) are immunosuppressive drugs. Both drugs significantly inhibit the activity of CN and have been widely used in clinical practice. However, CsA and FK506 need to bind to the corresponding ligands to exert their function. There are some unavoidable side effects in application, especially hepatotoxicity, nephrotoxicity and neurotoxicity. Therefore, it is very important to identify new CN inhibitors with low toxicity.

NFATs have two CN binding sites, including the PxIxIT motif and LxVP motif. In 1999, Aramburu *et al*. constructed combinatorial peptide libraries based on the NFAT-PxIxIT motif and the optimal peptide PVIVIT (MAGPHPVIVITGPHEE)[11] was selected. Experiments have shown that this fragment has a stronger binding ability with CN than the PxIxIT motifs of NFATs. This fragment binds to the A subunit of CN and dephosphorylation and translocation of NFAT were inhibited. The transcription and expression of immune-related genes downstream of NFAT are subsequently inhibited.

The LxVP motif in the NFAT family also plays an important role in the combination of CN and NFAT. According to research on the binding ability of each LxVP motif of NFAT with CN, the LxVP motif binds to the binding interface of CNA and CNB. This motif has also attracted the attention of researchers and can be used as a potential inhibitory sequence of the CN/NFAT pathway.

African swine fever virus (ASFV) is a large icosahedral double-stranded DNA virus. A238L is a protein inhibitor expressed by

CONTACT Jing Luo luojing@bnu.edu.cn Department of Biochemistry and Molecular Biology, Gene Engineering and Biotechnology, Beijing Key Laboratory, No.19, Xinjiekouwaidajie, Beijing Normal University, Beijing 100875, China; Zhimei Li lizm1211@163.com Department of Neurology, Beijing Tiantan Hospital, Capital Medical University, China National Clinical Research Center for Neurological Diseases, Beijing 100050, China
*The authors should be regarded as joint first authors.
†Present address: Junior High School Department, Shenzhen Senior High School Group East Campus, Shenzhen, Guangdong 518119, China

ASFV at the initial stage of infection. A238L expression in the host inhibits the CN/NFAT pathway and subsequently inhibits the host's immune response. Thus, immune evasion of ASFV is achieved[12,13]. The A238L protein includes a total of 238 amino acids. There are two binding motifs that can specifically bind to CN. The two motifs are linked by a 16-amino acid linker (GCEDNVYEKLPEQNSN).

We selected the optimised PVIVIT motif (GPHPVIVIT) and the YLAVP motif (YLAVPQHPYQWAK) from NFATc1 as the main components, used a 16-AA linker (GCEDNVYEKLPEQNSN) from A238L as the linker, and then designed a short peptide named pep4 with a full length of 38 amino acids. Compared with our previously published pep3[14], we replaced the EV motif from RCAN1 with the PVIVIT motif selected from the peptide library. Pep4 is 11 amino acids shorter than pep3. We used a series of experimental techniques and methods to explore the binding ability of pep4 to CN and its effect on the CN/NFAT signalling pathway.

Materials and methods

Cell culture and drug treatment

HEK293 cells and Jurkat cells were obtained from cryopreserved cells in the laboratory. HEK293 cells were cultured in DMEM medium (Gibco, USA) containing 10% FBS. Jurkat cells were cultured in RPMI 1640 medium (Gibco, USA) containing 10% FBS. All cells were grown in a humidified incubator with 5% CO_2 at 37 °C. CsA (2 μM) (Beyotime, China) was used to pretreat the cells for 1 h, and ionomycin (1 μM) (Beyotime, China) was used to stimulate the cells for 0.5 h.

Plasmid construction and transfection

The EGFP-pep4 plasmid was generated by cloning pep4 into the EGFP-C1 empty vector. GST-pep4 and its mutant were constructed using the pGEX-4T-1 empty vector. Plasmid DNA was transfected into cells with Lipofectamine 2000 (Invitrogen).

Western blotting

The cells and tissues were lysed with an appropriate amount of RIPA lysis solution (Applygen, China) containing protease inhibitors, PMSF, and β-ME. The proteins were separated by SDS-PAGE and then transferred to PVDF membranes for primary antibodies incubation and secondary antibodies incubation. Mouse anti-GFP and mouse anti-β-actin were purchased from Abbkine. Rabbit anti-calcineurin A, mouse anti-GST, and rabbit anti-NFAT1 were purchased from Cell Signalling Technology. Rabbit anti-lamin B1 was provided by Proteintech. Goat anti-mouse IgG and goat anti-rabbit IgG secondary antibodies were purchased from SGB-BIO. After the secondary antibody incubation was completed, ECL luminescent solution (Tanon, China) was used for colour development. A Tanon instrument was used to obtain images, and ImageJ was used for image analysis.

GST pull-down assay

GST fusion proteins were expressed in the BL21 *Escherichia coli* strain and obtained from the lysate (50 mM Tris-HCl, 0.1 mM PMSF, 2 mM DTT, 0.1% β-mercaptoethanol, and protease inhibitors). The lysate was centrifuged to obtain the supernatant. The supernatant was incubated with 50 μl 50% Glutathione-Sepharose 4B beads at 4 °C for 3 h and then washed 5 times with wash buffer (50 mM Tris-HCl). The mouse brain was lysed with lysis buffer (RIPA, 0.1 mM PMSF, 2 mM DTT, 0.1% β-mercaptoethanol, and protease inhibitors) to obtain crude CN. Then, 500 μl diluted mouse brain lysate (500 mg/μl) was added to the mixed solution, incubated at 4 °C for 1 h, and washed with wash buffer (50 mM Tris-HCl) 7 times. Finally, the samples were boiled in loading buffer and analysed by western blotting.

Co-immunoprecipitation assays

50 μl Protein A/G plus Agarose was incubated with the antibody at 4 °C for 2 h in buffer I (1× TBS, pH 7.6). Transfected HEK293 cells were treated with lysate (1× TBS, 0.1 mM PMSF, 2 mM DTT, 0.1% β-mercaptoethanol, 1 mM EDTA, 0.5% NP-40 pH 7.6, and protease inhibitors), and the supernatant was centrifuged. The supernatant was added to the corresponding mixture of Protein A/G plus Agarose and antibody and then incubated at 4 °C for 3 h. Finally, the samples were boiled in loading buffer and analysed by western blotting.

Immunofluorescence assay

Cells were cultivated (37 °C, 0.05% CO_2) on coverslips located on the bottom of the 12-well plates for 12 h. After incubation with FITC-11R-pep4 for 1 h, the cells were fixed with preprepared 4% paraformaldehyde (Applygen Technologies Inc. Beijing, China) at room temperature (RT) for 10 min and then permeated with 0.3% Triton X-100 in PBS for 10 min. The 5% BSA was diluted in PBS and incubated with cells at RT for 1 h. The cell nucleus was stained with 5 mg/ml Hoechst 33258 at RT for 10 min and incubated with an antifluorescence quencher. The coverslips were observed using a ZEISS LSM700 microscope system.

Flow cytometry

The incubated Jurkat cells were resuspended in 500 μl PBS and filtered through a flow cytometer tube to obtain a single cell suspension. Then, the cells were collected, and the cells with fluorescein (FITC)-conjugated peptide were counted using the ACEA Flow Cytometry System (NovoCyte).

Preparation of cytoplasmic and nuclear extracts

According to the instructions of the kit (Beyotime, China), the treated HEK293 cells were washed with PBS and collected. Then, cytoplasmic protein extraction reagent A containing PMSF (1 mM) was added. The mixture was vortexed at high speed for 5 s and placed on ice for 15 min. Then, cytoplasm extract reagent B was added to the solution. The mixture was vortexed at high speed for 5 s, placed in an ice bath for 1 min, and vortexed at high speed for 5 s. The supernatant, which contained the cytoplasmic protein, was centrifuged. Then, nuclear protein extraction reagent containing PMSF (1 mM) was added to the remaining nuclear pellets. The mixture was vortexed at high speed for 30 s, placed in an ice bath for 30 min, and centrifuged to obtain the supernatant, which contained the nuclear protein. The samples were analysed by western blotting.

RNA extraction and quantitative real-time PCR (qRT-PCR)

Total RNA was extracted from cells using the RNeasy Plus Mini Kit (Qiagen, China). Reverse transcription was performed using the

Takara PrimeScriptTM RT Reagent Kit. Real-time quantitative reverse transcription PCR (qRT-PCR) was performed using the ABI QuantStudio6 Flex full-function quantitative PCR instrument. β-actin served as a reference gene for qRT-PCR.

Constructing a mouse model of asthma and dosing

Twenty-four male BALB/C mice aged 6–8 weeks were purchased from Charles River. The animals were group-housed under the following laboratory conditions: temperature of 20 ± 1 °C, humidity of 40–60%, and 12:12-h light/dark cycle. Mice had free access to food and water throughout the course of the experiments. The animals were treated in accordance with the current law and the NIH Guide for Care and Use of Laboratory Animals. The protocol number of animal ethics evaluation in this study (CLS-EAW-2020–007) is approved by Ethic and Animal Welfare Committee, College of Life Science, Beijing Normal University.

The mice were randomly divided into 4 groups with 6 mice in each group. 10 μg OVA was injected intraperitoneally on the 7th and 14th days to provoke allergic reactions. Intranasal 1% OVA was administered from the 21st to 24th days to generate an acute asthma model. Before challenge, 11 R-pep4 (200 μg) was administered to the experimental group. In addition, 11 R-PVIVIT (200 μg) was used as a positive control, and physiological saline was used as a negative control. On the 25th day, the mice were anaesthetized with ether, and their lungs were obtained for section staining. All work was conducted with the formal approval of the animal care committee. All experimental procedures were approved by the Animal Ethics Committee of College of Life Sciences, Beijing Normal University.

Data analysis

We used identical settings and exported them to ImageJ (NIH) to obtain images for imaging analyses to quantitatively assess protein distributions. The data were analysed using GraphPad Prism 5 based on the means ± SEM. Statistical significance was determined by comparing the means of different groups and conditions using ANOVA followed by Tukey's test. $^{*}p < 0.05$, $^{**}p < 0.01$, $^{***}p < 0.001$.

Results

Pep4 has strong binding ability to both endogenous and exogenous CN

Pep4 is composed of pep1s (PVIVIT), linker and pep2 (NFATc1-LxVP). We compared the CN binding ability of pep4 with that of two single binding motifs. The GST pull-down results showed that the binding ability of pep4 with CN was stronger than that of a single binding motif (Figure 1(A,B)). We performed site-directed mutations of the main CN binding sites in pep4 (Figure 1(C)). The first mutation (Mutant 1) changed pep4-PVIVIT (pep1s) to pep4-PAIAIT, and the second mutation (Mutant 2) changed pep4-YLAVP (pep2) to pep4-YAAAA. The third mutation (Mutant 3) is the combination of the first two mutations. Using GST pull-down assay, we compared the CN binding ability of pep4 with three mutants. The results showed that the mutations in PVIVIT, YLAVP or both affected the binding of pep4 to CN (Figure 1(D,E)). It is obvious that the key amino acids in the two binding motifs are mutated, which has a significant impact on the binding force between pep4 and CN. This finding indicated that the binding sites in pep4 were consistent with our expected design and that the corresponding binding regions on CN could be identified.

We not only verified the binding ability between pep4 and CN *in vitro* but also verified the binding ability between pep4 and endogenous CN in HEK293 cells. We transfected 4 μg EGFP-pep4 plasmids into HEK293 cells. After 24 h, we stimulated the cells with ionomycin (1 μM) for 0.5 h. The immunoprecipitation results showed that EGFP-pep4 binds to endogenous CN in HEK293 cells (Figure 1(F)).

We also compared the CN binding ability of A238L, pep3, and pep4. The GST pull-down experiment was performed using the CN from mouse brain. The results showed that there was no significant difference in the CN binding ability of pep4 compared with pep3 (composed of RCAN1-EV, linker, NFATc1-LxVP) and A238L, and all three peptides exhibit strong CN binding ability (Figure 1(G,H)).

Li et al. reported that the binding constant K_d of PVIVIT with CN is approximately 0.5 μM. Carme Mulero et al. used the fluorescence polarisation method to obtain a binding constant K_d of approximately 1.25 μM for the RCAN1-EV motif with CN. The binding constants of PVIVIT and RCAN1-EV are on the micromolar levels, and the difference is not significant. Our experimental results also showed that the two artificial peptides exhibited similar binding ability to CN.

Pep4 significantly inhibits purified CN activity

Pep4 specifically binds to CN and inhibits the activity of CN by occupying the corresponding binding site of CN. We used RII (DLDVPIPGRFDRRVpSVAAE) as the substrate to detect the effect of pep4 on CN enzyme activity *in vitro* based on malachite green colorimetry. Given that CN is highly expressed in the brain, we used the protein extract of the mouse brain as the crude enzyme extract. The synthesised peptide pep4 was incubated with the crude extract of mouse brain enzyme, and the substrate RII was added for the dephosphorylation reaction. Finally, malachite green was added for colour development. The results showed that pep4 inhibited CN enzyme activity in a dose-dependent manner (Figure 2(A)). The IC_{50} of pep4 was 5.1 nM, indicating that pep4 had a strong inhibitory effect on CN.

To compare the effect on the CN enzyme activity of pep4 and its single binding motif, we measured the activity of CN with pep1s, pep2 and pep4 at the same concentration of 25 nM. We found that pep1s and pep2 had minimal effects on CN activity, but pep4 significantly inhibits CN activity (Figure 2(B)).

We also explored the type of inhibition mediated by pep4. A fixed concentration of pep4 was incubated with a concentration gradient of RII to determine the enzyme activity. The CN enzyme kinetic curves were plotted with or without pep4 (Figure 2(C)). Comparing the kinetic curves of CN with or without pep4, we found that the V_{max} values of the two groups were very close, whereas the K_m of the pep4 group increased significantly (Table 1). These results showed that pep4 inhibited CN enzyme activity through competitive inhibition.

Pep4 effectively targets the CN/NFAT pathway

Normal cells can only allow a small number of lipid soluble, nonpolar or uncharged molecules to enter and exit freely. In 2004, Noguchi et al. first linked polyarginine (11 R)[15] to the short peptide PVIVIT and successfully realised the efficient entry of the short peptide into the cell. The peptide exhibited proper physiological function in the cell. We also linked 11 R to the N-terminus of pep4

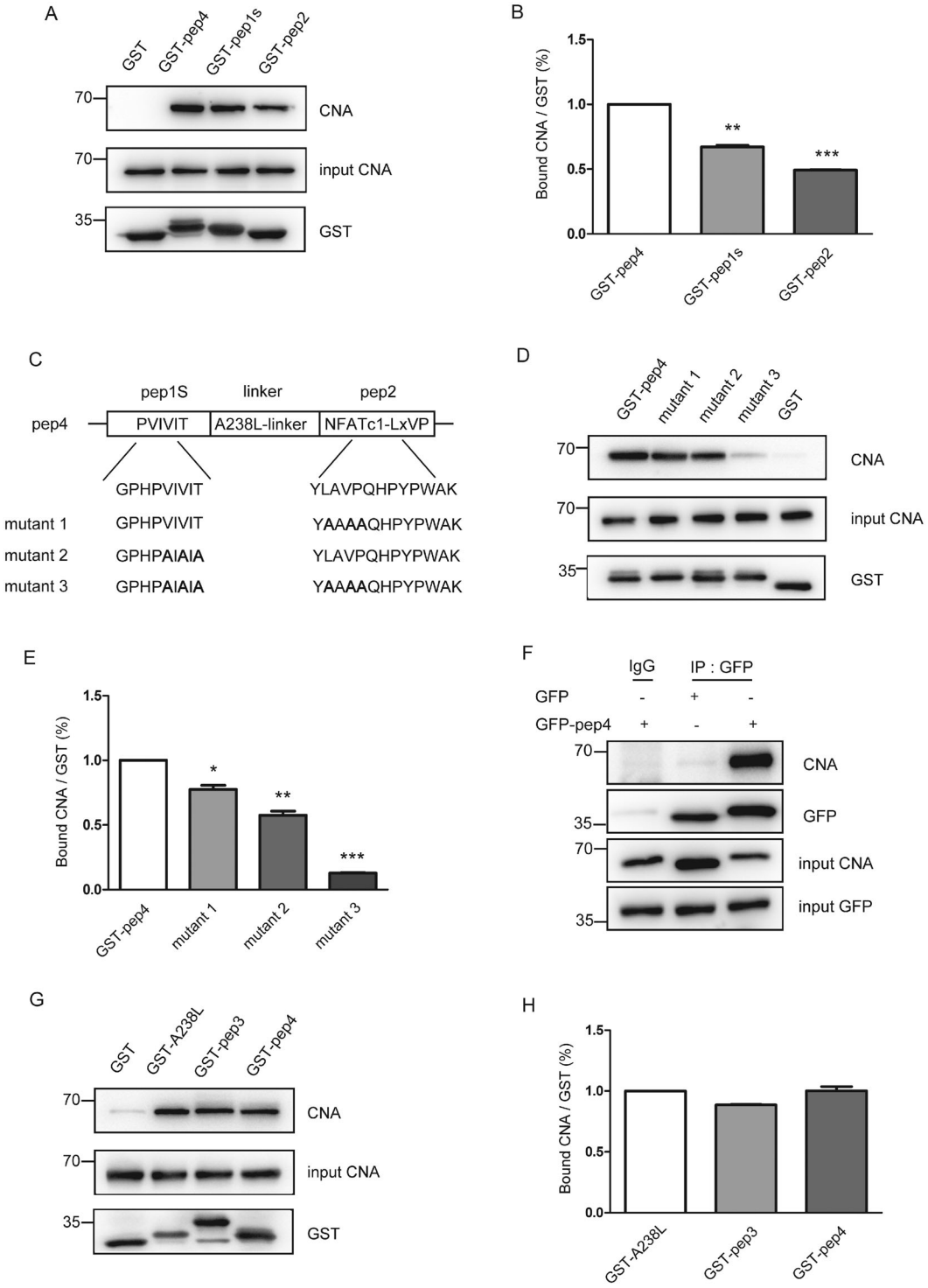

Figure 1. Pep4 strongly binds CN. (A) Pep4 binds CNA from mouse brain lysates in GST pull-down assays. GST-pep4, GST-pep1s, and GST-pep2 were incubated with CN from the mouse brain, CN monoclonal antibody was used to observe the combined CN by western blotting (upper panel), and the same amount of mouse brain lysates was added to each group middle panel). Western blotting was performed on the fusion protein with GST antibody to confirm the amount of GST-fusion protein added in each group (bottom panel). (B) The optical density of CN bound to pep4, pep1s, and pep2 was measured. The histogram reflects the relative ability of combining CN. Data are presented as the mean ± SEM of three independent experiments. $^{**}p < 0.01$ and $^{***}p < 0.001$ compared with the pep4 group. (C) Schematic diagram of pep4 and its mutants. Pep4 is composed of pep1s, linker and pep2. The important binding sites of pep1s and pep2 were mutated to obtain mutants 1, 2 and 3. (D) Pep4 and its mutants bind CNA from mouse brain lysates in GST pull-down assays. The pull-down experiment was performed under the same experimental conditions as B. (E) The optical density of the CN bound to pep4 and its mutants was determined. The histogram reflects the relative ability of combining CN. Data are presented as the mean ± SEM of three independent experiments. $^{*}p < 0.05$, $^{**}p < 0.01$ and $^{***}p < 0.001$ compared with the pep4 group. (F) The binding of pep4 to endogenous CN in HEK293 cells. GFP empty plasmids or GFP-pep4 plasmids were transfected into HEK293 cells for 24 hours. The cell lysate was subjected to immunoprecipitation experiments with GFP antibody. The final lysate was subjected to western blotting detection, and CN monoclonal antibody was used to detect the binding of CN in each group. The IgG group and GFP group serve as negative controls. (G) A238L, pep3 and pep4 bind CNA from mouse brain lysates in GST pull-down assays. The pull-down experiment was performed under the same experimental conditions as B and D. (H) The optical density of the CN bound to A238L, pep3 and pep4 was determined. The histogram reflects the relative ability of combining CN. Data are presented as the mean ± SEM of three independent experiments.

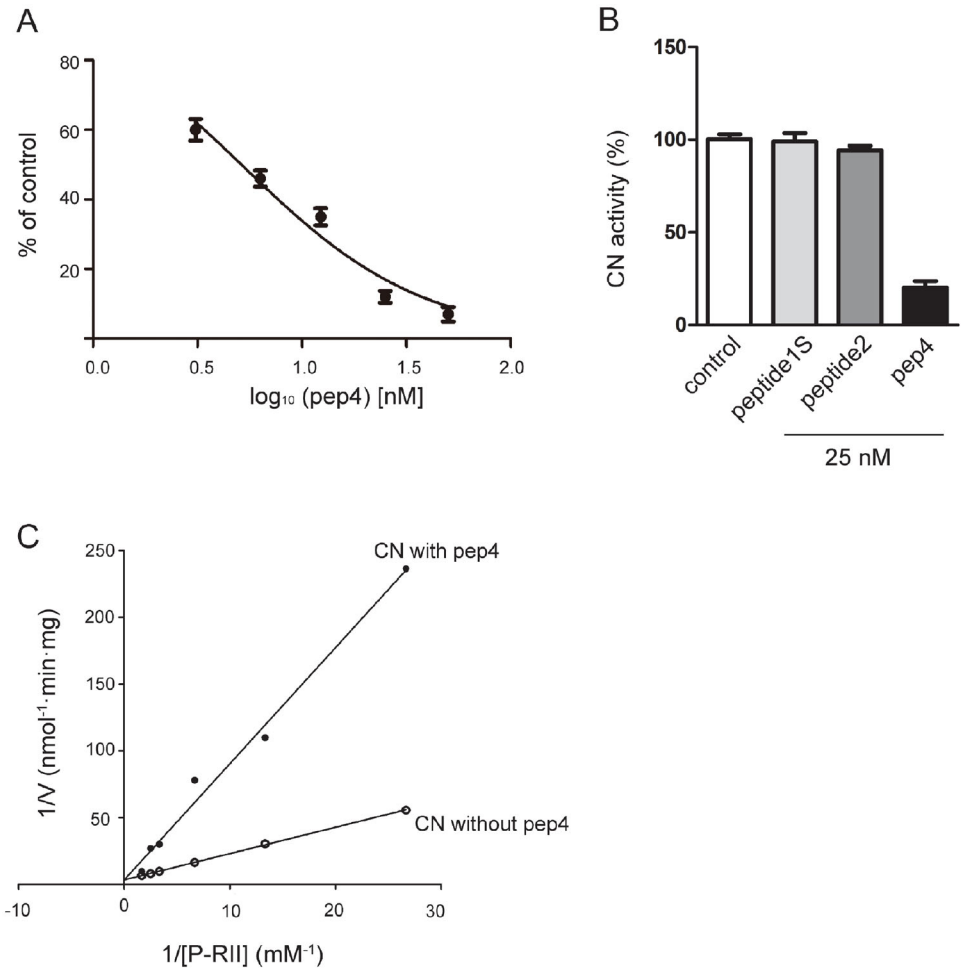

Figure 2. Pep4 competitively inhibits the enzymatic activity of CN. (A) The effect of pep4 on CN enzyme activity in the mouse brain. The horizontal axis represents the concentration of pep4, and the vertical axis represents the inhibition degree of enzyme activity. (B) The effect of pep4 and its single binding motif on CN enzyme activity. Pep1s, pep2 or pep4 at the same concentration of 25 nM were incubated to detect the enzyme activity of CN. The horizontal axis represents the different short peptides, and the vertical axis represents the enzyme activity of CN. (C) Kinetic analysis of CN in brain extracts with or without pep4. Lineweaver-Burk plots of activity against substrate concentration in mouse brain extracts.

Table 1. Kinetic parameters of CN in brain extracts with or without pep4.

	V_{max} (nmol·min^{-1}·mg^{-1})	K_m (mmol/L)
CN	0.30 ± 0.03	0.59 ± 0.02
Pep4 + CN	0.32 ± 0.03	2.80 ± 0.22

The values reported are the average of at least three independent determinations with the standard error of the mean.

to enhance its ability to enter cells. To observe whether 11 R-pep4 entered the cells, FITC was used for fluorescence labelling.

To explore whether 11 R-pep4 successfully enters the cell and determine the timeline of its entry, we incubated Jurkat cells with FITC-11R-pep4 and set the incubation time gradient (1–14 h). Immunofluorescence staining showed that FITC-11R-pep4 successfully entered the cells and was evenly distributed in the cytoplasm (Figure 3(A)). We collected 20,000 cells and analysed the fluorescence intensity using flow cytometry. The results showed that when the peptide was incubated for 1 h, the average fluorescence intensity of the cells reached a high level and was maintained for approximately 7 h. After 7 h, the fluorescence intensity gradually decreased (Figure 3(B,C)). We hypothesised that this was due to the degradation of short peptides in cells. We incubated Jurkat cells with different concentrations of FITC-11R-pep4 (1–10 μM) for 6 h. We collected 20,000 cells and analysed the fluorescence intensity by flow cytometry. Compared with the blank control group, the fluorescence intensity increased with increasing peptide concentrations in a concentration-dependent manner (Figure 3(D)). These results indicated that FITC-11R-pep4 can enter the cells successfully and remain stable in the cells for a certain period of time.

It has been reported that the charge of polypeptides may affect their ability to penetrate the cell membrane. According to the dissociation constant pK_a of the amino acid side chain, we roughly calculated that pep3 has more negative charges than pep4. However, 11 arginine modifications make both peptides positively charged. From our observations, minimal differences in the ability of the two peptides to penetrate the cell membrane were noted.

After being dephosphorylated by CN, NFAT enters the nucleus and binds to downstream immune-related genes, thereby activating the immune response. Pep4 exhibits strong binding ability with CN. Pep4 inhibits the binding of CN and NFAT by occupying the binding site of CN and NFAT. Thus, the dephosphorylation and nuclear translocation of NFAT was inhibited. We verified the ability of pep4 to prevent NFAT from entering the nucleus in HEK293 cells. We transfected 4 μg EGFP-pep4 plasmids into

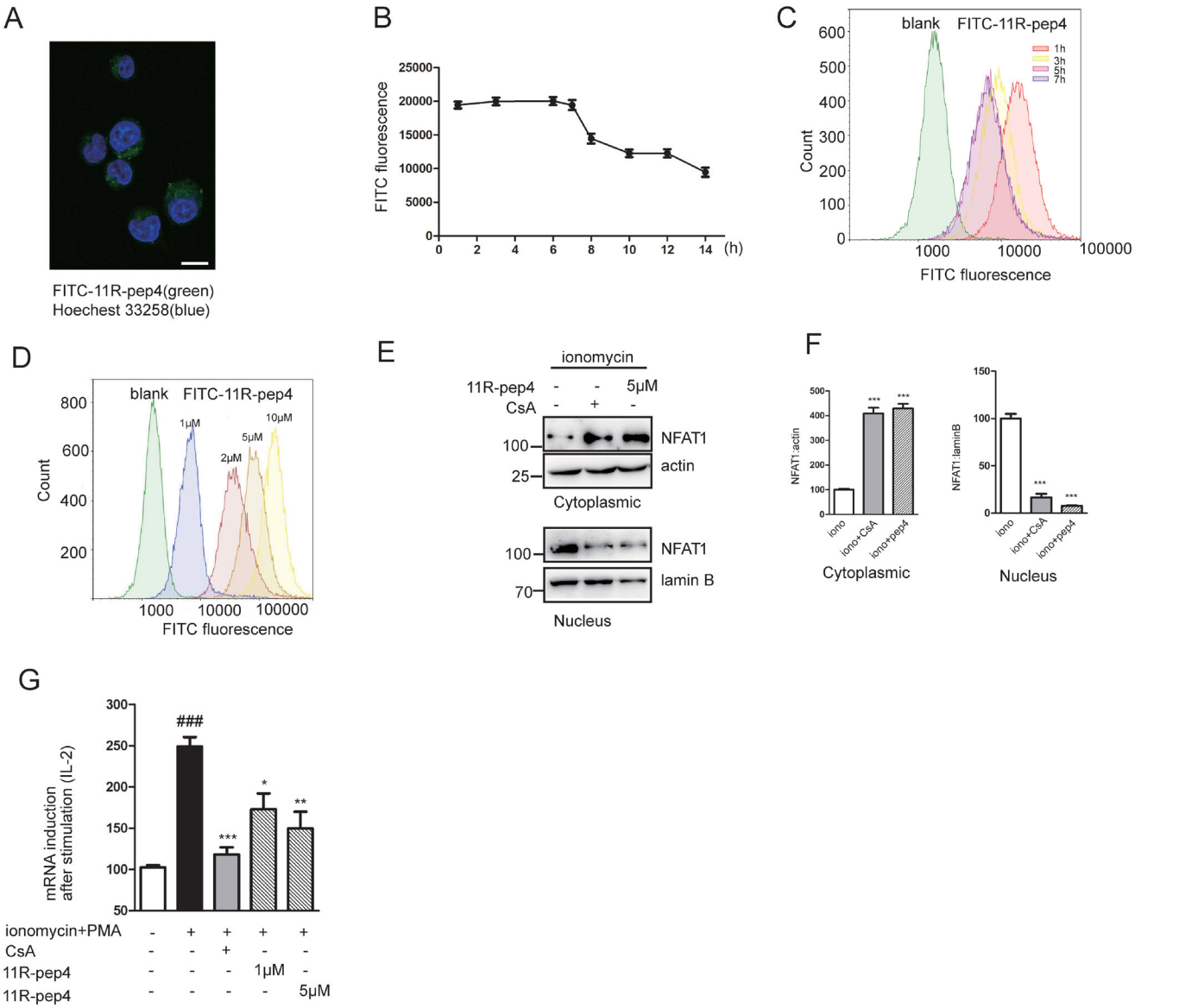

Figure 3. Cell-permeable pep4 can block the ionomycin-induced nuclear translocation of NFAT1 and the gene expression of the CN/NFAT downstream pathway. (A) Immunofluorescence staining of Jurkat cells incubated with FITC-11R-pep4. Green represents FITC-11R-pep4. The nucleus is stained with Hoechst 33258. Scale bar, 10 μm. (B) The curve between incubation time and fluorescence intensity of FITC-11R-pep4. Incubation time is 1–14 h. (C) Average fluorescence intensity of FITC-11R-pep4 at different incubation times determined by flow cytometry. The incubation times were 1, 3, 5 and 7 h. (D) Average fluorescence intensity of FITC-11R-pep4 at different concentrations after 6 h incubation by flow cytometry. The concentrations of FITC-11R-pep4 were 1, 2, 5, and 10 μM. (E) 11R-pep4 inhibits NFAT1 from entering the nucleus. HEK293 cells are incubated with 11R-pep4. The nuclei and cytoplasm of HEK293 cells were separated and analysed by western blotting. NFAT1 monoclonal antibody was used to detect the amount of NFAT1 in the nucleus and cytoplasm, and β-actin and lamin B1 were used as the loading controls. CsA served as the positive control. (F) The optical density of NFAT1 in the cytoplasm and nucleus was measured. The histogram reflects the relative content of NFAT1 in each group. Data are presented as the mean ± SEM of three independent experiments; $^{***}p < 0.001$ compared with the ionomycin group. (G) 11R-pep4 inhibits *IL-2* mRNA expression. Jurkat cells were pre-treated with different concentrations of 11R-pep4 and stimulated with 1 μM ionomycin and 50 mg/mL PMA. Total RNA was extracted for quantitative real-time PCR to detect the mRNA expression of the *IL-2* gene, and CsA served as the positive control.

HEK293 cells and separated the nuclear and cytoplasmic NFAT1 fractions. The results showed that pep4 can effectively inhibit NFAT1 from entering the nucleus, and similar inhibitory effects were noted of the positive control drug CsA (2 μM) (Figure 3(E)).

To explore whether pep4 can achieve an immunosuppressive effect, we chose to assess IL-2, which is the downstream expression factor of the CN/NFAT signalling pathway. We incubated Jurkat cells with 11 R-pep4 and detected *IL-2* mRNA expression by RT-PCR. When the concentration of pep4 was 1 μM and 5 μM, *IL-2* mRNA expression was significantly inhibited (Figure 3(G)). These results indicated that 11 R-pep4 exerts a relatively stable biological effect in the cell. Moreover, 11 R-pep4 inhibits CN from activating NFAT. Then the expression of downstream cytokines subsequently decreased, and the immune response was influenced.

11R-pep4 improves the airway pathological characteristics in OVA-induced asthmatic mice

To further explore the role of 11 R-pep4 in the body, we evaluated the physiological effects of 11 R-pep4 on the tracheal inflammatory response in a mouse asthma model. We established a mouse model of asthma and administered 11 R-PVIVIT and 11 R-pep4. Here, 11 R-PVIVIT served as the positive control 10 (Figure 4(A)).

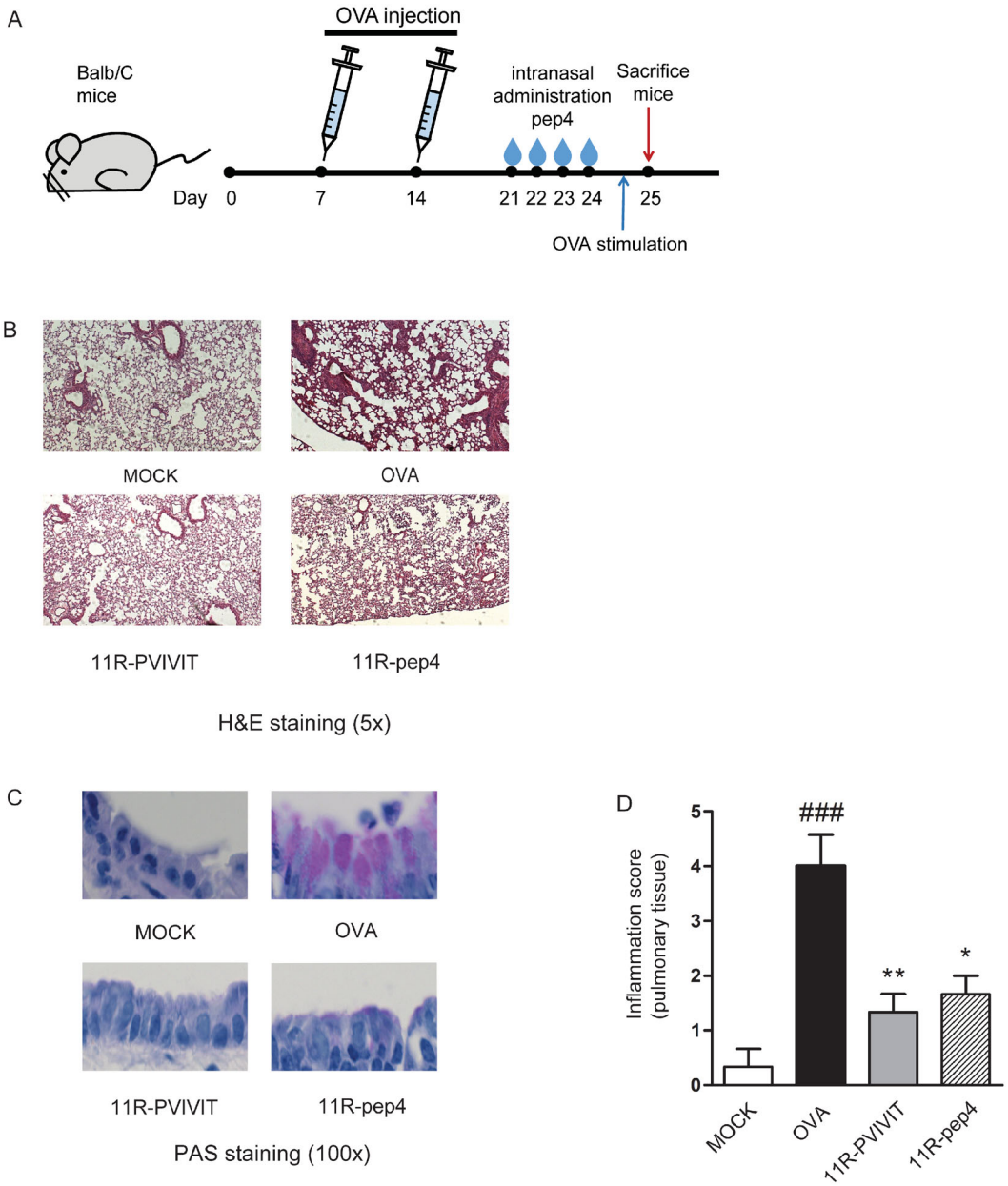

Figure 4. 11 R-pep4 can alleviate the inflammatory response in asthmatic mice. (A) Schematic diagram of the mouse asthma experimental design. Male BALB/c mice were selected and sensitised by intraperitoneal injection of 10 μg OVA on the 7th and 14th days. Mice were challenged with 1% OVA for four consecutive days from the 21st day to construct an acute asthma model. Then, 11R-pep4 was administered before each OVA challenge. The mice were sacrificed on the 25th day for analysis. (B) Lung tissue was prepared for histological analysis, including morphology and the infiltration of inflammatory cells, by H&E staining. Representative results of H&E staining in the four groups are shown. Scale bar, 200 μm. (C) Lung tissue was prepared for histological analysis. PAS-stained airway cross-sections of each group are shown. Scale, 10 μm. (D) Inflammatory changes were graded by histopathological assessment using a semiquantitative scale of 0–5. The results are presented as the mean ± S.E.M. for each group ($n = 4$). $^{*}p < 0.01$ and $^{**}p < 0.001$ compared with the OVA group. $^{###}p < 0.001$ compared with the mock group.

We obtained the mice lungs to observe inflammation (Figure 4(B)). Compared with the normal group, the OVA group exhibited obvious infiltration of inflammatory cells, and the tracheal wall was thickened. The tracheal mucosa exhibited high levels of secretion, and eosinophils were visible. In the 11 R-PVIVIT group and 11 R-pep4 group, the inflammatory status was improved, only a small number of inflammatory cells infiltrated, and no obvious thickening of the tracheal wall or eosinophils appeared. PAS staining (Figure 4(C)) showed that the number of goblet cells in the OVA group was significantly increased, indicating a severe inflammatory reaction. Administration of 11 R-pep4 reduced the inflammatory reaction. These results indicated that 11 R-pep4 can also exert its immunosuppressive effect at the animal level.

Discussion

The CN/NFAT pathway plays an important role in various physiological processes, including T cell activation, which is conducive to the immune response. However, in some special cases, such as allergic reactions, autoimmune diseases, and organ transplantation, immunity needs to be suppressed. CsA and tacrolimus are classical CN inhibitors and are currently the most effective immunosuppressive drugs in clinical application[16,17]. They play an immunosuppressive role by binding their respective intracellular ligands cyclosphilin (CyP) and FK506 binding protein (FKBP). Because CyP and FKBP still have their own physiological functions, CsA and FK506 have some side effects, such as nephrotoxicity[18,19],

neurotoxicity, and hypertension[20]. Therefore, the development of new immunosuppressive drugs is highly desirable.

In our previous studies, we focussed on screening small molecule inhibitors of CN. We used CN as a target enzyme to screen its inhibitors and identified some small molecule compounds, such as quercetin[21], kaempferol[22], and isogarcinol[23,24]. For example, isogarcinol inhibits the activity of CN *in vitro* and has an immunosuppressive effect on experimental autoimmune encephalomyelitis. Compared with CsA, this compound has fewer adverse effects in experimental animals. However, how isogarcinol exerts its immunosuppressive effect, especially its effect on the downstream NFAT signalling pathway, needs to be further explored.

In addition to the focus on enzyme activity, there have been an increasing number of studies on the interaction between CN and NFAT in recent years. Protein-protein interactions[25] are widely found in biological systems controlling diverse cellular events. These interactions are implicated in many diseases, such as neurodegenerative diseases[26] and cancer[27]. Regulation of protein-protein interactions provides ideal targets for drug intervention. For example, disruption of the interaction between CN and NFAT may block the immune response associated with this signalling pathway. NFAT has two binding motifs that bind to CN: the PxIxIT motif and the LxVP motif. Noguchi first designed a cell-permeable PVIVIT peptide. This peptide affects the binding of CN and the NFAT-PxIxIT motif and the subsequent immune response.

Compared with small molecule inhibitors, peptide inhibitors that destroy the interaction between CN and NFAT exhibit clearer effects. We think that active peptides have more advantages than small molecule drugs in the design of drugs to disrupt CN-NFAT interactions. Using the combination of CN and NFAT-LxVP as an example, many discontinuous amino acid residues from the two proteins play a key role in the interaction, such as Y, L and V from the NFAT-LxVP motif and F352, W363, and Y351 from CN. Low molecular weight compounds are difficult to use to prevent this substantial high affinity interaction. In this respect, Cheng et al. reported[28] that the design of small molecular inhibitors for protein-protein interactions remains challenging. The greatest difficulty faced by scientists is that the interface between the protein and small molecule is approximately 300–1000 Å, but the contact surface of the protein-protein interaction is 1500–3000 Å. Furthermore, some small molecule inhibitors have inhibitory effects on protein-protein interactions *in vitro*, but they have little or no activity in tissue culture. In addition, many inhibitors are not sufficiently specific. Therefore, the mechanism by which small molecule inhibitors affect protein-protein interactions *in vivo* remains worthy of further study.

Peptides designed according to protein-protein interactions offer great advantages in the specificity of targets. We designed a bioactive peptide (named pep3) against the CN/NFAT interaction that has two binding sites derived from the RCAN1-PxIxIT motif and the NFATc1-LxVP motif. Cell-permeable 11-arginine-modified pep3 (11 R-pep3) blocks the NFAT downstream signalling pathway and immune response *in vivo*. In this study, we replaced the RCAN1-EV motif with the PVIVIT peptide to study the effect of this peptide on the CN/NFAT signalling pathway. Although pep4 exhibits stronger enzymatic inhibition than pep3, its effects on the subsequent signalling pathway and *in vivo* immunosuppression are basically the same as that noted for pep3.

Most peptides exhibit good water solubility, so they do not easily penetrate the lipid bilayer of cells[29]. Peptides need to be modified by transmembrane peptides to enter cells. We used polyarginine[30,31] to modify pep4. FITC-labelled 11 R-pep4 was observed as a fluorescent signal in all living Jurkat cells. FITC fluorescence was visualised in the cytoplasm. We also observed the fluorescence intensity in the time course and dose-dependent experiments. Our results also showed that the fluorescence intensity of FITC-labelled 11 R-pep4 decreased by half in approximately 8 h. These intracellular data remind us that pep4 as a peptide inhibitor still has some unavoidable problems, such as its chemical and metabolic stability. The modification and optimisation of pep4 need to be strengthened in the future research.

In general, our results show that pep4 has a strong CN binding ability and inhibitory effect on CN both intracellularly and extracellularly and competitively inhibits the binding of CN and NFAT. Pep4 inhibits NFAT1 dephosphorylation and nuclear translocation, thus inhibiting the expression of downstream immune-related factors and finally achieving the goal of immunosuppression. These findings will contribute to the discovery of new CN inhibitors and promising immunosuppressive drugs.

Disclosure statement

We confirm that this work is original and has not been published elsewhere, nor is it currently under consideration for publication elsewhere. We have no conflicts of interest to disclose.

Funding

The present work was supported by the National Natural Science Foundation of China [Project 82074056].

References

1. Guerini D. Calcineurin: not just a simple protein phosphatase. Biochem Biophys Res Commun 1997;235:271–5.
2. Perrino BA. Regulation of calcineurin phosphatase activity by its autoinhibitory domain. Arch Biochem Biophys 1999; 372:159–65.
3. Li H, Rao A, Hogan PG. Interaction of calcineurin with substrates and targeting proteins. Trends Cell Biol 2011;21: 91–103.
4. Macián F, López-Rodríguez C, Rao A. Partners in transcription: NFAT and AP-1. Oncogene 2001;20:2476–89.
5. Klee CB, Ren H, Wang X. Regulation of the calmodulin-stimulated protein phosphatase, calcineurin. J Biol Chem 1998;273:13367–70.
6. Li SJ, Wang J, Ma L, et al. Cooperative autoinhibition and multi-level activation mechanisms of calcineurin. Cell Res 2016;26:336–49.
7. Shou J, Jing J, Xie J, et al. Nuclear factor of activated T cells in cancer development and treatment. Cancer Lett 2015;361: 174–84.
8. Medyouf H, Ghysdael J. The calcineurin/NFAT signaling pathway: a novel therapeutic target in leukemia and solid tumors. Cell Cycle 2008;7:297–303.
9. Kipanyula MJ, Kimaro WH, Seke Etet PF. The emerging roles of the calcineurin-nuclear factor of activated T-lymphocytes pathway in nervous system functions and diseases. J Aging Res 2016;2016:5081021.
10. Sitara D, Aliprantis AO. Transcriptional regulation of bone and joint remodeling by NFAT. Immunol Rev 2010;233: 286–300.
11. Aramburu J, Yaffe MB, López-Rodríguez C, et al. Affinity-driven peptide selection of an NFAT inhibitor more selective than cyclosporin A. Science 1999;285:2129–33.

12. Grigoriu S, Bond R, Cossio P, et al. The molecular mechanism of substrate engagement and immunosuppressant inhibition of calcineurin. PLoS Biol 2013;11:e1001492.
13. Granja AG, Nogal ML, Hurtado C, et al. The viral protein A238L inhibits cyclooxygenase-2 expression through a nuclear factor of activated T cell-dependent transactivation pathway. J Biol Chem 2004;279:53736–46.
14. Wang L, Cheng N, Wang P, et al. A novel peptide exerts potent immunosuppression by blocking the two-site interaction of NFAT with calcineurin. J Biol Chem 2020;295: 2760–70.
15. Noguchi H, Matsushita M, Okitsu T, et al. A new cell-permeable peptide allows successful allogeneic islet transplantation in mice. Nat Med 2004;10:305–9.
16. Kahan BD. Cyclosporine: a revolution in transplantation. Transplant Proc 1999;31:14S–5S.
17. Kiani A, Rao A, Aramburu J. Manipulating immune responses with immunosuppressive agents that target NFAT. Immunity 2000;12:359–72.
18. Benigni A, Bruzzi I, Mister M, et al. Nature and mediators of renal lesions in kidney transplant patients given cyclosporine for more than one year. Kidney Int 1999;55:674–85.
19. Ganesan V, Milford DV, Taylor CM, et al. Cyclosporin-related nephrotoxicity in children with nephrotic syndrome[J]. Pediatr Nephrol 2002;17:225–6.
20. Mihatsch MJ, Kyo M, Morozumi K, et al. The side-effects of ciclosporine-A and tacrolimus. Clin Nephrol 1998;49: 356–63.
21. Wang H, Zhou CL, Lei H, Wei Q. Inhibition of calcineurin by quercetin in vitro and in Jurkat cells. J Biochem 2010;147: 185–90.
22. Wang H, Zhou CL, Lei H, et al. Kaempferol: a new immunosuppressant of calcineurin. IUBMB Life 2008;60:549–54.
23. Wang M, Xie Y, Zhong Y, et al. Amelioration of Experimental Autoimmune Encephalomyelitis by Isogarcinol Extracted from Garcinia mangostana L. Mangosteen. J Agric Food Chem 2016;64:9012–21.
24. Cen J, Wang M, Jiang G, et al. The new immunosuppressant, isogarcinol, binds directly to its target enzyme calcineurin, unlike cyclosporin A and tacrolimus. Biochimie 2015;111: 119–24.
25. Uvebrant K, da Graça Thrige D, Rosén A, et al. Discovery of selective small-molecule CD80 inhibitors. J Biomol Screen 2007;12:464–72.
26. Ganeshpurkar A, Swetha R, Kumar D, et al. Protein-Protein Interactions and Aggregation Inhibitors in Alzheimer's Disease. Curr Top Med Chem 2019;19:501–33.
27. Sharma SK, Ramsey TM, Bair KW. Protein-protein interactions: lessons learned. Curr Med Chem Anticancer Agents 2002;2:311–30.
28. Cheng AC, Coleman RG, Smyth KT, et al. Structure-based maximal affinity model predicts small-molecule druggability. Nat Biotechnol 2007;25:71–5.
29. Futaki S. Arginine-rich peptides: potential for intracellular delivery of macromolecules and the mystery of the translocation mechanisms. Int J Pharm 2002;245:1–7.
30. Mitchell DJ, Kim DT, Steinman L, et al. Polyarginine enters cells more efficiently than other polycationic homopolymers. J Pept Res 2000;56:318–25.
31. Gonçalves E, Kitas E, Seelig J. Binding of oligoarginine to membrane lipids and heparan sulfate: structural and thermodynamic characterization of a cell-penetrating peptide. Biochemistry 2005;44:2692–702.